AAS 21-235

ANALYTICAL DESCRIPTION OF RELATIVE POSITION AND VELOCITY ON J2-PERTURBED ECCENTRIC ORBITS

Matthew Willis* **and Simone D'Amico†**

A new solution is introduced for the relative position and velocity of two spacecraft on eccentric orbits perturbed by Earth oblateness. The equations of relative motion subject to an arbitrary perturbing force are derived and this general framework is used to develop a partial solution for the case of perturbation by the second zonal harmonic of Earth's gravitational potential. The performance of the new solution is compared with several prominent solutions from the literature, and the inability of variation of parameters to produce a complete, closed-form solution for the J_2 corrections is discussed.

INTRODUCTION

Accurate and efficient models for the relative motion of two or more spacecraft in Earth orbit are needed to enable potential commercial and scientific applications ranging from on-orbit inspection and servicing of satellites to observations of gravitational waves and direct imaging of extrasolar planets.[1] Increased interest in such distributed space systems, combined with the limited processing power typical of flight hardware has driven recent research in the area of analytical solutions to the equations of relative motion. Such models are particularly valuable because their accuracy is not tied to an integration step size or iteration tolerance and they are therefore practical for onboard implementation. Sullivan and D'Amico conducted a thorough survey of existing dynamics models and solutions, including a comparison of their performance under various assumptions.[2] Relative motion models may be broadly divided between two categories based on the choice of state variables. Orbital element representations offer better accuracy due to their fundamental connection to the underlying physics and relative motion geometry. However, spacecraft sensors and actuators do not directly measure or affect the orbital elements, so there is an advantage to using translational state models that avoid the intermediate representation. The present work builds upon the long history and large body of work focused on analytical modeling of the relative position and velocity vectors, but has close connections to approaches based on relative orbit elements (ROE).

The development of analytical, translational state solutions dates back to the seminal work of Clohessy and Wiltshire (CW) at the beginning of the space age.[3] They addressed the linear, time-invariant problem of relative motion between two spacecraft in close proximity on near-circular orbits. A second-order solution to the circular orbit problem was independently derived by London and Sasaki and later by Stringer and Newman, and is often referred to as the Quadratic-Volterra solution.[4–7] These solutions were generated using the method of successive approximations, wherein the first-order CW solution is substituted into the nonlinear dynamics, resulting in a linear, inhomogeneous system that may be solved by elementary differential equations techniques. The same

*PhD Candidate, Department of Aeronautics and Astronautics, Stanford University, 496 Lomita Mall, Stanford, CA 94305.
†Professor, Department of Aeronautics and Astronautics, Stanford University, 496 Lomita Mall, Stanford, CA 94305.

strategy has been used more recently by Melton and Butcher, et al. to incorporate leading-order effects of eccentricity.[8,9] A more accurate description of the linear dynamics governing relative motion on elliptical orbits was introduced by Tschauner and Hempel (TH), through appropriate normalization of the coordinates and use of the true anomaly as the independent variable.[10] Solutions to this system by Tschauner and Hempel, Carter, and others offered better accuracy than the CW solution in slightly eccentric orbits but suffered from singularities at zero eccentricity.[11] Yamanaka and Ankersen (YA) were able to remove this singularity with the use of a new integral that grows in proportion to time.[12] Ogundele and Agboola introduced a power series solution in true anomaly for the elliptical orbit dynamics, with a systematic method for computing higher-order terms. Recently, Willis, Lovell, and D'Amico (WLD) introduced a second-order solution for relative motion on eccentric orbits by applying the method of successive approximations to the first-order YA solution.[13] Subsequent work by the authors developed the corresponding second-order solution in Curvilinear coordinates.[14] A primary motivation for developing such higher-order solutions is their potential utility for resolving the range ambiguity for angles-only relative navigation.[15] However, this application is sensitive to modeling errors introduced by perturbations as well as to higher-order Keplerian effects.[16] The present work addresses this limitation by establishing a framework for incorporating the effects of perturbing forces into higher-order solutions.

Although linear models describing unperturbed motion are ubiquitous in spacecraft formation flying studies, many forces in the space environment cause deviations from such idealized dynamics. Principal among these are the effects of Earth oblateness, atmospheric drag, solar radiation pressure, and tidal forces from the Sun and Moon.[17] Much of the relative dynamics modeling effort of the last two decades has been focused on addressing such perturbations. The Gim-Alfriend state transition matrix (STM), widely regarded as the state of the art, bridges the gap between state representation categories.[18] It uses a linear mapping of the chief's orbital elements to a spherical coordinate system to account for the effects of Earth oblateness and atmospheric drag on the relative motion of nearby spacecraft. Other authors have preferred to work more exclusively with one state representation or another. Koenig, et al. have exploited the physical insights offered by ROE to develop STMs that handle all of the major forces affecting satellites orbiting Earth.[19] More recently, Kuiack and Ulrich built upon earlier work by Gurfil and others to develop a nonlinear orbital elements-based solution that includes J_2 perturbations.[20,21] The simplest translational state model is that due to Schweighart and Sedwick, which linearizes and averages the J_2 perturbation for near-circular orbits to achieve a linear, time-invariant system analogous to CW.[22,23] However, this simplicity is accomplished at the expense of accuracy. Biria and Russell used the Vinti theory of satellite motion to develop a translational state model that incorporates the effects of J_2 and J_3.[24] The present work builds most directly on the effort by Butcher and Burnett et al. to add J_2 corrections to their higher-order solutions for circular and slightly eccentric orbits.[25,26] While a similar approach is taken, their solution is based on CW and treats eccentricity only approximately while this work seeks to fully incorporate eccentricity effects in the model.

The body of this paper is divided into three sections. First, the YA solution and method of successive approximations are reviewed. Next a general strategy is developed for incorporating perturbation effects into the higher-order solutions, emphasizing how these effects enter into the equations of motion. The framework is applied to modeling the effect of Earth oblateness on the relative dynamics and developing a partial analytical solution to the disturbance equations. This model is then validated against numerical integration and compared with several related models. The paper concludes with a summary of key results and directions for future research.

BACKGROUND

Equations of Motion in Cartesian Coordinates

Before introducing the perturbing equations, it is important to review the development of the higher-order equations of motion and the solution methodology. In any coordinate system, we may express the motion of a deputy spacecraft relative to a chief spacecraft in terms of the position vector $\mathbf{r}$ from the central body to the chief and the relative position vector $\boldsymbol{\delta}\mathbf{r}$ from the chief to the deputy. The deputy's fundamental orbital differential equation may then be written as

$$ {}^{I}\ddot{\mathbf{r}} + {}^{I}\boldsymbol{\delta}\ddot{\mathbf{r}} = -\mu\frac{\mathbf{r}+\boldsymbol{\delta}\mathbf{r}}{\|\mathbf{r}+\boldsymbol{\delta}\mathbf{r}\|^3} \tag{1} $$

where ${}^{I}(\dot{})$ indicates a time derivative with respect to an inertial frame and μ is the gravity parameter of the central body. To isolate $\boldsymbol{\delta}\mathbf{r}$, we assume that $\delta r \ll r$ and expand $\|\mathbf{r}+\boldsymbol{\delta}\mathbf{r}\|^3$ using a binomial series. Truncating at second order in $(\delta r/r)$, the right-hand side of Equation (1) becomes

$$ -\mu\frac{\mathbf{r}+\boldsymbol{\delta}\mathbf{r}}{\|\mathbf{r}+\boldsymbol{\delta}\mathbf{r}\|^3} \approx -\frac{\mu}{r^3}\left(\mathbf{r}+\boldsymbol{\delta}\mathbf{r} - 3\frac{\mathbf{r}\cdot\boldsymbol{\delta}\mathbf{r}}{r^2}(\mathbf{r}+\boldsymbol{\delta}\mathbf{r}) - \frac{3}{2}\frac{\delta r^2}{r^2}\mathbf{r} + \frac{15}{2}\frac{(\mathbf{r}\cdot\boldsymbol{\delta}\mathbf{r})^2}{r^4}\mathbf{r}\right) \tag{2} $$

The first term in the series expansion is the acceleration ${}^{I}\ddot{\mathbf{r}}$ of the chief in the inertial frame and can be subtracted from both sides of Equation (1). When working with Cartesian coordinates, we express the relative motion with respect to the Hill frame rotating with the chief's orbit. Let ${}^{L}(\dot{})$ denote a time derivative with respect to this rotating frame, $\boldsymbol{\delta}\mathbf{v} \equiv {}^{L}\boldsymbol{\delta}\dot{\mathbf{r}}$ be the relative velocity, and $\boldsymbol{\omega}$ be the angular velocity of the rotating frame with respect to the inertial frame. Applying the theorem of Coriolis and using the fact that ${}^{I}\dot{\boldsymbol{\omega}} = {}^{L}\dot{\boldsymbol{\omega}} = \dot{\boldsymbol{\omega}}$, we obtain the equations of relative motion to second order in spacecraft separation,

$$ {}^{L}\boldsymbol{\delta}\ddot{\mathbf{r}} = -\frac{\mu}{r^3}\left(\boldsymbol{\delta}\mathbf{r} - 3\frac{\mathbf{r}\cdot\boldsymbol{\delta}\mathbf{r}}{r^2}(\mathbf{r}+\boldsymbol{\delta}\mathbf{r}) - \frac{3}{2}\frac{\delta r^2}{r^2}\mathbf{r} + \frac{15}{2}\frac{(\mathbf{r}\cdot\boldsymbol{\delta}\mathbf{r})^2}{r^4}\mathbf{r}\right) - 2\boldsymbol{\omega}\times\boldsymbol{\delta}\mathbf{v} - \dot{\boldsymbol{\omega}}\times\boldsymbol{\delta}\mathbf{r} - \boldsymbol{\omega}\times\boldsymbol{\omega}\times\boldsymbol{\delta}\mathbf{r} \tag{3} $$

The terms in parentheses approximate the differential gravitational force on the two spacecraft while those outside the parentheses describe the fictitious forces arising from the rotating reference frame.

To make the equations amenable to solution for eccentric orbits, the independent variable is changed from time to true anomaly f, and the coordinates are normalized by the chief's orbit radius. For convenience, we introduce the parameter

$$ k = \frac{p}{r} = 1 + e\cos f \tag{4} $$

where $p = a(1-e^2)$ is the semi-latus rectum. We will denote the normalized coordinates with $\tilde{(\,)}$ and derivatives with respect to true anomaly by $(\,)'$. The transformed relative position $\boldsymbol{\delta}\tilde{\mathbf{r}}$ and relative velocity $\boldsymbol{\delta}\tilde{\mathbf{v}} \equiv {}^{L}\boldsymbol{\delta}\tilde{\mathbf{r}}'$ are related to $\boldsymbol{\delta}\mathbf{r}$ and $\boldsymbol{\delta}\mathbf{v}$ by

$$ \begin{aligned} \boldsymbol{\delta}\tilde{\mathbf{r}} &= \frac{1}{r}\boldsymbol{\delta}\mathbf{r} \\ \boldsymbol{\delta}\tilde{\mathbf{v}} &= -\frac{e}{p}\boldsymbol{\delta}\mathbf{r}\sin f + \frac{1}{k}\sqrt{\frac{p}{\mu}}\boldsymbol{\delta}\mathbf{v} \end{aligned} \tag{5} $$

$$ \begin{aligned} \boldsymbol{\delta}\mathbf{r} &= r\boldsymbol{\delta}\tilde{\mathbf{r}} \\ \boldsymbol{\delta}\mathbf{v} &= \sqrt{\frac{\mu}{p}}\left(e\boldsymbol{\delta}\tilde{\mathbf{r}}\sin f + k\boldsymbol{\delta}\tilde{\mathbf{v}}\right) \end{aligned} \tag{6} $$

Equations (1) through (6) are in coordinate-independent vector form. The relative motion is often described in the radial-transverse-normal (RTN) coordinate frame of the chief, also referred to as the local-vertical-local-horizontal frame. The RTN coordinates are centered on the chief and defined with the x-axis directed away from the Earth, the z-axis parallel to the chief's orbital angular momentum, and the y-axis completing the right-handed triad. The relative position vector is therefore $\boldsymbol{\delta}\mathbf{r} = [x, y, z]^T$. After applying the appropriate transformations in this coordinate system, the second-order equations of motion take the form

$$\begin{aligned} \tilde{x}'' - 2\tilde{y}' - \frac{3}{k}\tilde{x} &= -\frac{3}{k}\tilde{x}^2 + \frac{3}{2k}(\tilde{y}^2 + \tilde{z}^2) \\ \tilde{y}'' + 2\tilde{x}' &= \frac{3}{k}\tilde{x}\tilde{y} \\ \tilde{z}'' + \tilde{z} &= \frac{3}{k}\tilde{x}\tilde{z} \end{aligned} \tag{7}$$

In Equation (7), the first-order terms that appear in the TH equations have been moved to the left while the nonlinear second-order terms remain on the right-hand side.

Yamanaka-Ankersen Solution

Yamanaka and Ankersen found an analytical solution to the linear system of equations obtained by dropping the right-hand side of Equation (7),

$$\begin{aligned} \tilde{x}'' - 2\tilde{y}' - \frac{3}{k}\tilde{x} &= 0 \\ \tilde{y}'' + 2\tilde{x}' &= 0 \\ \tilde{z}'' + \tilde{z} &= 0 \end{aligned} \tag{8}$$

Their key contribution was to eliminate singularities in the solution to the TH equations by introducing the integral $J(t)$, defined as

$$J(t) = \int_{f_0}^{f} \frac{d\tau}{k(\tau)^2} = \sqrt{\frac{\mu}{p^3}}(t - t_0) \tag{9}$$

Although the integration is taken over true anomaly, $J(t)$ is a linear function of time. The solution to Equation (8) is given by the linear system

$$\begin{bmatrix} \tilde{x} \\ \tilde{y} \\ \tilde{z} \\ \tilde{x}' \\ \tilde{y}' \\ \tilde{z}' \end{bmatrix} = \begin{bmatrix} \left(1 - \frac{3}{2}ekJ(t)\sin f\right) & k\sin f & k\cos f & 0 & 0 & 0 \\ -\frac{3}{2}k^2 J(t) & (1+k)\cos f & -(1+k)\sin f & 1 & 0 & 0 \\ 0 & 0 & 0 & 0 & \sin f & \cos f \\ -\frac{3}{2}e\left((k\sin f)'J(t) + \frac{\sin f}{k}\right) & (k\sin f)' & (k\cos f)' & 0 & 0 & 0 \\ \frac{3}{2}(2ekJ(t)\sin f - 1) & -2k\sin f & e - 2k\cos f & 0 & 0 & 0 \\ 0 & 0 & 0 & 0 & \cos f & -\sin f \end{bmatrix} \begin{bmatrix} K_1 \\ K_2 \\ K_3 \\ K_4 \\ K_5 \\ K_6 \end{bmatrix} \tag{10}$$

where $(k\sin f)' = \cos f + e\cos 2f$ and $(k\cos f)' = -(\sin f + e\sin 2f)$. The integration constants K_1 through K_6 characterize the relative motion geometry and are closely related to the ROE.[27]

To express the solution in terms of initial conditions, one may solve for the integration constants vector $\mathbf{K}$ by inverting Equation (10) and evaluating at the initial time t_0. Using $J(t_0) = 0$, this

leads to

$$\begin{bmatrix} K_1 \\ K_2 \\ K_3 \\ K_4 \\ K_5 \\ K_6 \end{bmatrix} = \begin{bmatrix} \frac{6k_0+2e^2-2}{1-e^2} & 0 & 0 & \frac{2ek_0\sin f_0}{1-e^2} & \frac{2k_0^2}{1-e^2} & 0 \\ -3\left(1+\frac{e^2}{k_0}\right)\frac{\sin f_0}{1-e^2} & 0 & 0 & \frac{k_0\cos f_0-2e}{1-e^2} & -\frac{1+k_0}{1-e^2}\sin f_0 & 0 \\ -3\frac{e+\cos f_0}{1-e^2} & 0 & 0 & -\frac{k_0\sin f_0}{1-e^2} & -\frac{e+(1+k_0)\cos f_0}{1-e^2} & 0 \\ -3e\left(1+\frac{1}{k_0}\right)\frac{\sin f_0}{1-e^2} & 1 & 0 & \frac{ek_0\cos f_0-2}{1-e^2} & -e\frac{1+k_0}{1-e^2}\sin f_0 & 0 \\ 0 & 0 & \sin f_0 & 0 & 0 & \cos f_0 \\ 0 & 0 & \cos f_0 & 0 & 0 & -\sin f_0 \end{bmatrix} \begin{bmatrix} \tilde{x} \\ \tilde{y} \\ \tilde{z} \\ \tilde{x}' \\ \tilde{y}' \\ \tilde{z}' \end{bmatrix}_0 \tag{11}$$

The product of the matrices in Equations (10) and (11) is the famous YA STM for relative motion on eccentric orbits. In the limit as eccentricity approaches zero, $k \to 1$, $J(t) \to n(t-t_0)$, $f \to n(t-t_{ref})$, and Equations (10) and (11) reduce to the CW solution for near-circular orbits.

Solution Methodology

Higher-order solutions to the equations of relative motion may be found by treating the true solution as a series expansion

$$\boldsymbol{\delta\tilde{\mathbf{r}}} = \boldsymbol{\delta\tilde{\mathbf{r}}}_1 + \boldsymbol{\delta\tilde{\mathbf{r}}}_2 + \boldsymbol{\delta\tilde{\mathbf{r}}}_3 + \cdots \tag{12}$$

in which $\boldsymbol{\delta\tilde{\mathbf{r}}}_1$ captures effects up to $\mathcal{O}(\delta r/r)$, $\boldsymbol{\delta\tilde{\mathbf{r}}}_2$ captures effects up to $\mathcal{O}(\delta r^2/r^2)$, and so forth. The first-order solution $\boldsymbol{\delta\tilde{\mathbf{r}}}_1$ to the rectilinear dynamics in Equation (7) is precisely the YA solution in Equation (10). For convenience, the initial conditions of $\boldsymbol{\delta\tilde{\mathbf{r}}}_i$ and $\boldsymbol{\delta\tilde{\mathbf{r}}}_i'$ are chosen to be zero for $i > 1$. The first-order solution is therefore exact at the initial state, i.e. $\boldsymbol{\delta\tilde{\mathbf{r}}}(f_0) \equiv \boldsymbol{\delta\tilde{\mathbf{r}}}_1(f_0)$, and the higher-order components correct for the accumulation of error in the first-order solution. This assumption is beneficial because it allows use of Equation (11) to define the integration constants K_1 through K_6 without having to invert a higher-order system.

To derive the second-order solution $\boldsymbol{\delta\tilde{\mathbf{r}}}_2$, we substitute Equation (12) into the equations of motion and expand in products of $\boldsymbol{\delta\tilde{\mathbf{r}}}_i$ components. The only terms in the expansion that contribute to the $\boldsymbol{\delta\tilde{\mathbf{r}}}_2$ solution are those that are linear in $\boldsymbol{\delta\tilde{\mathbf{r}}}_2$ or quadratic in $\boldsymbol{\delta\tilde{\mathbf{r}}}_1$. Terms involving products of $\boldsymbol{\delta\tilde{\mathbf{r}}}_1$ and $\boldsymbol{\delta\tilde{\mathbf{r}}}_2$ components will contribute to $\boldsymbol{\delta\tilde{\mathbf{r}}}_3$ and terms quadratic in $\boldsymbol{\delta\tilde{\mathbf{r}}}_2$ will contribute to $\boldsymbol{\delta\tilde{\mathbf{r}}}_4$. Higher-order effects due to terms truncated in the derivation of Equation (7) from Equation (3) will be at least $\mathcal{O}(\delta r^3/r^3)$ and have no contribution to $\boldsymbol{\delta\tilde{\mathbf{r}}}_2$. Thus, the second-order components solve the system formed by substituting the first-order solution into the nonlinear terms on the right-hand side of Equation (7),

$$\begin{aligned} \tilde{x}_2'' - \frac{3}{k}\tilde{x}_2 - 2\tilde{y}_2' &= RHS_x(f) = -\frac{3}{k}\tilde{x}_1^2 + \frac{3}{2k}(\tilde{y}_1^2 + \tilde{z}_1^2) \\ \tilde{y}_2'' + 2\tilde{x}_2' &= RHS_y(f) = \frac{3}{k}\tilde{x}_1\tilde{y}_1 \\ \tilde{z}_2'' + \tilde{z}_2 &= RHS_z(f) = \frac{3}{k}\tilde{x}_1\tilde{z}_1 \end{aligned} \tag{13}$$

where the functions $RHS_j(f)$ have been introduced for generality.

The system in Equation (13) simplifies the dynamics of Equation (7) by decoupling the out-of-plane component $\tilde{z}_2$ from the in-plane components $\tilde{x}_2$ and $\tilde{y}_2$. The latter can be decoupled by

integrating the $\tilde{y}_2''$ equation once to obtain the system,

$$\begin{aligned} \tilde{x}_2'' - \frac{3}{k}\tilde{x}_2 - 2\tilde{y}_2' &= RHS_x(f) \\ \tilde{y}_2' &= -2\tilde{x}_2 + \int RHS_y(f)df + c_{y1} \end{aligned} \tag{14}$$

where the constant of integration c_{y1} has been explicitly removed from the integral on the right-hand side. Applying the zero initial conditions to $\tilde{y}_2'$ and $\tilde{x}_2$, we find that $c_{y1} = -3\int(\tilde{x}_1\tilde{y}_1/k)df|_{f_0}$. Substituting the expression for $\tilde{y}_2'$ into the first equation leads to a second-order linear inhomogeneous ODE for $\tilde{x}_2$,

$$\tilde{x}_2'' + \left(4 - \frac{3}{k}\right)\tilde{x}_2 = RHS_x(f) + 2\int RHS_y(f)df + 2c_{y1} \tag{15}$$

Second-order components of the relative motion appear only on the left of Equation (15), while the right may be written as an explicit function of f using Equation (10).

Equation (15) can be solved by variation of parameters if two linearly independent solutions are available for the homogeneous equation[28]

$$\tilde{x}_2'' + \left(4 - \frac{3}{k}\right)\tilde{x}_2 = 0 \tag{16}$$

Because the higher-order terms involving $\tilde{x}_1$ and $\tilde{y}_1$ do not appear in the homogeneous equation, it is identical to that obtained from the TH equations. The solutions to this equation introduced by Yamanaka and Ankersen are

$$\begin{aligned} \varphi_1 &= k\sin f \\ \varphi_2 &= 3e^2kJ(t)\sin f + k\cos f - 2e \end{aligned} \tag{17}$$

and their linear independence was demonstrated in that work.[12] The particular solution φ_p to any inhomogeneous equation formed by placing an arbitrary function $RHS(f)$ of the independent variable on the right of Equation (16) can be found using the variation of parameters formula,

$$\varphi_p = \varphi_1\int\frac{\varphi_2 RHS(f)}{1-e^2}df - \varphi_2\int\frac{\varphi_1 RHS(f)}{1-e^2}df \tag{18}$$

where the Wronskian in the denominator is $\varphi_1'\varphi_2 - \varphi_1\varphi_2' = 1 - e^2$. By superposition, the general solution is the sum of the particular solution and a linear combination of the homogeneous solutions φ_1 and φ_2:

$$\tilde{x}_2 = c_{x1}\varphi_1 + c_{x2}\varphi_2 + \varphi_p \tag{19}$$

We use Equations (10), (15), (17), (18), (19), and the zero initial conditions to solve for the second-order correction $\tilde{x}_2$ to the relative motion in the radial direction. The correction $\tilde{y}_2$ in the along-track direction is found by direct integration of the second line of Equation (14) using the solution for $\tilde{x}_2$ and zero initial conditions. Finally, applying the variation of parameters procedure to the third line of Equation (13) using the homogeneous solutions $\varphi_1 = \sin f$ and $\varphi_2 = \cos f$, and $\varphi_1'\varphi_2 - \varphi_1\varphi_2' = 1$, results in the out-of-plane correction $\tilde{z}_2$. While this procedure has been described for the unperturbed dynamics of Equation (7) in this section, the methodology generalizes to the perturbed case.

MODELING PERTURBATIONS

Many forces other than point-mass gravity act on objects in orbit, including higher-order geopotential effects, atmospheric drag, solar radiation pressure, and tidal effects from third bodies. The method of successive approximations outlined in the previous section can be generalized to correct for these effects. In addition to presenting a framework for handling general perturbations, this section examines the specific case of acceleration due to the J_2 harmonic of the Earth's gravitational potential. For spacecraft in low Earth orbit, the effect J_2 can be comparable to the nonlinear corrections due to inter-spacecraft separation that were modeled in Equation (13). Thus, only the leading-order corrections for the perturbation will be addressed.

Argument of Latitude Formulation

Before delving into the disturbance equations, recall that our second-order solutions are built upon YA and use the chief's true anomaly as the independent variable. This is a geometric quantity that must be computed from the spacecraft position and velocity through the eccentricity vector. For near-circular orbits, the eccentricity vector is small and easily affected by perturbations, causing large variations in the argument of perigee ω and true anomaly f. As a result, the true anomaly is a poor choice for modeling the dynamics and, more practically, a difficult quantity to know in orbit. To avoid this problem, we will reformulate the YA solution in terms of the argument of latitude $u = \omega + f$. Unlike true anomaly, the argument of latitude is weakly affected by perturbations. It is therefore easier to estimate, and provides a more stable foundation for the dynamics model.

For unperturbed orbits, ω is constant and $du = df$. Because these derivatives are interchangeable, the equations of relative motion are unchanged by the change of variable and the previously derived solutions can be used with the substitution $f \rightarrow u - \omega$. The explicit dependence on ω may be removed by recasting the solution in terms of the eccentricity vector components $e_x = e\cos\omega$ and $e_y = e\sin\omega$. With these substitutions, the parameter k becomes

$$k = 1 + e_x \cos u + e_y \sin u \tag{20}$$

and the homogeneous solutions to Equation (16) are

$$\begin{aligned} \psi_1 &= k\sin u - 2e_y\left(1 + \frac{3}{2}kk'J(t)\right) \\ \psi_2 &= k\cos u - 2e_x\left(1 + \frac{3}{2}kk'J(t)\right) \end{aligned} \tag{21}$$

where $k' = -e_x\sin u + e_y\cos u$. Solving the TH equations with ψ_1 and ψ_2 leads to

$$\begin{bmatrix} \tilde{x} \\ \tilde{y} \\ \tilde{z} \\ \tilde{x}' \\ \tilde{y}' \\ \tilde{z}' \end{bmatrix} = \begin{bmatrix} \left(1+\frac{3}{2}kk'J(t)\right) & k\sin u & k\cos u & 0 & 0 & 0 \\ -\frac{3}{2}k^2J(t) & (1+k)\cos u & -(1+k)\sin u & 1 & 0 & 0 \\ 0 & 0 & 0 & 0 & \sin u & \cos u \\ -\frac{3}{2}\left((k'^2 + k(1-k))J(t) + \frac{k'}{k}\right) & (k\sin u)' & (k\cos u)' & 0 & 0 & 0 \\ -\frac{3}{2}(2kk'J(t)+1) & -\sin u + (k\cos u)' & -\cos u - (k\sin u)' & 0 & 0 & 0 \\ 0 & 0 & 0 & 0 & \cos u & -\sin u \end{bmatrix} \begin{bmatrix} K_1 \\ K_2 \\ K_3 \\ K_4 \\ K_5 \\ K_6 \end{bmatrix} \tag{22}$$

where $(k\sin u)' = \cos u + e_x\cos 2u + e_y\sin 2u$ and $(k\cos u)' = -\sin u - e_x\sin 2u + e_y\cos 2u$. Equation (22) is a formulation of the YA solution not found elsewhere in the literature and is equiv-

alent to Equation (10) with the constants K_i rotated by ω according to

$$\begin{bmatrix} K_1 \\ K_2 \\ K_3 \\ K_4 \\ K_5 \\ K_6 \end{bmatrix}_f = \begin{bmatrix} 1 & 0 & 0 & 0 & 0 & 0 \\ 0 & \cos\omega & -\sin\omega & 0 & 0 & 0 \\ 0 & \sin\omega & \cos\omega & 0 & 0 & 0 \\ 0 & 0 & 0 & 1 & 0 & 0 \\ 0 & 0 & 0 & 0 & \cos\omega & -\sin\omega \\ 0 & 0 & 0 & 0 & \sin\omega & \cos\omega \end{bmatrix} \begin{bmatrix} K_1 \\ K_2 \\ K_3 \\ K_4 \\ K_5 \\ K_6 \end{bmatrix}_u \tag{23}$$

From here on, $\mathbf{K} = [K_1, K_2, K_3, K_4, K_5, K_6]^T$ will only be used in reference to $\mathbf{K}_u$ and the subscript will be dropped. For completeness, the inverse matrix used to solve for $\mathbf{K}$ from the initial conditions is

$$\begin{bmatrix} K_1 \\ K_2 \\ K_3 \\ K_4 \\ K_5 \\ K_6 \end{bmatrix} = \begin{bmatrix} \frac{6k_0-2(1-e^2)}{1-e^2} & 0 & 0 & \frac{-2k_0k_0'}{1-e^2} & \frac{2k_0^2}{1-e^2} & 0 \\ -3\frac{e_y+(k_0+e^2)\sin u_0}{k_0(1-e^2)} & 0 & 0 & \frac{-2e_x+k_0\cos u_0}{1-e^2} & -\frac{e_y+(1+k_0)\sin u_0}{1-e^2} & 0 \\ -3\frac{e_x+(k_0+e^2)\cos u_0}{k_0(1-e^2)} & 0 & 0 & \frac{2e_y-k_0\sin u_0}{1-e^2} & -\frac{e_x+(1+k_0)\cos u_0}{1-e^2} & 0 \\ -3\frac{k_0'(1+k_0)}{k_0(1-e^2)} & 1 & 0 & \frac{(1+k_0)(k_0-2)}{1-e^2} & \frac{k_0'(1+k_0)}{1-e^2} & 0 \\ 0 & 0 & \sin u_0 & 0 & 0 & \cos u_0 \\ 0 & 0 & \cos u_0 & 0 & 0 & -\sin u_0 \end{bmatrix} \begin{bmatrix} \tilde{x} \\ \tilde{y} \\ \tilde{z} \\ \tilde{x}' \\ \tilde{y}' \\ \tilde{z}' \end{bmatrix}_0 \tag{24}$$

Equations of Motion

Following the successive approximations procedure of the previous section, the equations of motion are first expanded in the state variables and truncated at leading order in the perturbation. Next the first-order solution in Equation (22) is substituted into the perturbation terms, resulting in a linear, inhomogeneous system of the form

$$\begin{aligned} \tilde{x}_2'' - \frac{3}{k}\tilde{x}_2 - 2\tilde{y}_2' &= -\frac{3}{k}\tilde{x}_1^2 + \frac{3}{2k}(\tilde{y}_1^2 + \tilde{z}_1^2) + d_x(u) \\ \tilde{y}_2'' + 2\tilde{x}_2' &= \frac{3}{k}\tilde{x}_1\tilde{y}_1 + d_y(u) \\ \tilde{z}_2'' + \tilde{z}_2 &= \frac{3}{k}\tilde{x}_1\tilde{z}_1 + d_z(u) \end{aligned} \tag{25}$$

where the corrections needed to account for perturbations are modeled by $d_x(u)$, $d_y(u)$, and $d_z(u)$. This system can be solved by the variation of parameters method laid out in Equations (16) through (19), using the homogeneous solutions in Equation (21). The linearity of the system allows us to develop the second-order Keplerian corrections and first-order perturbation corrections separately and combine the solutions via superposition. Henceforth, the second-order terms will be omitted from the derivation, with the understanding that their solution can be added to that of the perturbation model.

A disturbance force produces leading-order effects on the system dynamics through several avenues, some with obvious physical significance and others with subtle mathematical interpretation. The following subsections examine each of these individually and provide the disturbance equations arising from J_2 perturbation.

Differential Force The most physically intuitive manifestation of the disturbance is the relative inertial acceleration caused by its differential action on the chief and deputy. Recall from Equation (1) that the acceleration of a spacecraft in an inertial reference frame is equal to the sum of the point-mass gravitational attraction to the central body and the perturbations $\mathbf{f}$ not modeled by Keplerian motion. Subtracting the motion of the chief and deputy in the inertial frame leads to the differential acceleration

$$ {}^{I}\boldsymbol{\delta}\ddot{\mathbf{r}} = -\mu\left(\frac{\mathbf{r}+\boldsymbol{\delta}\mathbf{r}}{\|\mathbf{r}+\boldsymbol{\delta}\mathbf{r}\|^3} - \frac{\mathbf{r}}{r^3}\right) + \mathbf{f}_d - \mathbf{f}_c \tag{26} $$

The term in parentheses was approximated through a binomial series expansion in the derivation of Equation (7), so the contribution of the disturbance force to the differential inertial acceleration is $\mathbf{d}_I = \mathbf{f}_d - \mathbf{f}_c$.

The second zonal harmonic J_2 of the gravitational potential produces an acceleration governed by

$$ \mathbf{f}_{J_2} = \frac{-\mu J_2 R_E^2}{2r^5}\left(6(\hat{\mathbf{Z}}\cdot\mathbf{r})\hat{\mathbf{Z}} + \left(3 - 15\frac{(\hat{\mathbf{Z}}\cdot\mathbf{r})^2}{r^2}\right)\mathbf{r}\right) \tag{27} $$

where R_E is Earth's equatorial radius and $\hat{\mathbf{Z}}$ is the unit vector parallel to Earth's rotation axis (not to be confused with the z-axis aligned with the chief's angular velocity vector). Expressed in the satellite's RTN coordinate system, this becomes

$$ \mathbf{f}_{J_2} = -\frac{3\mu J_2 R_E^2}{2r^4}\begin{bmatrix} 1 - 3\sin^2 i \sin^2 u \\ 2\sin^2 i \sin u \cos u \\ 2\sin i \cos i \sin u \end{bmatrix} \tag{28} $$

Using $\mathbf{r}_d = \mathbf{r} + \boldsymbol{\delta}\mathbf{r}$, taking the difference in forces acting on chief and deputy, and truncating at first order in $(\delta r/r)$, we obtain

$$ \begin{aligned} \mathbf{d}_I \approx -\frac{\mu J_2 R_E^2}{2r^4}\Bigg[&\left(3 - 15\frac{(\hat{\mathbf{Z}}\cdot\mathbf{r})^2}{r^2}\right)\frac{\boldsymbol{\delta}\mathbf{r}}{r} + 6\left(-5\frac{(\mathbf{r}\cdot\boldsymbol{\delta}\mathbf{r})(\hat{\mathbf{Z}}\cdot\mathbf{r})}{r^3} + \frac{\hat{\mathbf{Z}}\cdot\boldsymbol{\delta}\mathbf{r}}{r}\right)\hat{\mathbf{Z}} \\ &+ \left(-15\frac{\mathbf{r}\cdot\boldsymbol{\delta}\mathbf{r}}{r^2} - 15\left(\frac{2(\hat{\mathbf{Z}}\cdot\mathbf{r})(\hat{\mathbf{Z}}\cdot\boldsymbol{\delta}\mathbf{r})}{r^2} - 7\frac{\mathbf{r}\cdot\boldsymbol{\delta}\mathbf{r}}{r^4}(\hat{\mathbf{Z}}\cdot\mathbf{r})^2\right)\right)\frac{\mathbf{r}}{r}\Bigg] \end{aligned} \tag{29} $$

Making the appropriate substitutions for $\mathbf{r}$, $\boldsymbol{\delta}\mathbf{r}$, and $\hat{\mathbf{Z}}$ in RTN coordinates,

$$ \begin{aligned} \mathbf{d}_I\cdot\hat{\mathbf{R}} &= -\frac{6\mu J_2 R_E^2}{r^5}\left(-z\sin u\sin 2i - 2y\cos u\sin u\sin^2 i + x(3\sin^2 i\sin^2 u - 1)\right) \\ \mathbf{d}_I\cdot\hat{\mathbf{T}} &= -\frac{3\mu J_2 R_E^2}{2r^5}\left(z\cos u\sin 2i - 8x\cos u\sin u\sin^2 i + y(1+\sin^2 i(7\cos^2 u - 5))\right) \\ \mathbf{d}_I\cdot\hat{\mathbf{N}} &= -\frac{3\mu J_2 R_E^2}{2r^5}\left(y\cos u\sin 2i - 4x\sin u\sin 2i + z(3+\sin^2 i(5\cos^2 u - 7))\right) \end{aligned} \tag{30} $$

Performing the coordinate transformation and change of variables in Equation (6), then substituting

the first-order solution leads to the disturbance functions

$$
\begin{aligned}
d_{x,I}(u) &= -\frac{6J_2R_E^2}{p^2}k\left(-\tilde{z}_1\sin u\sin 2i - 2\tilde{y}_1\cos u\sin u\sin^2 i + \tilde{x}_1(3\sin^2 i\sin^2 u - 1)\right)\\
d_{y,I}(u) &= -\frac{3J_2R_E^2}{2p^2}k\left(\tilde{z}_1\cos u\sin 2i - 8\tilde{x}_1\cos u\sin u\sin^2 i + \tilde{y}_1(1+\sin^2 i(7\cos^2 u - 5))\right)\\
d_{z,I}(u) &= -\frac{3J_2R_E^2}{2p^2}k\left(\tilde{y}_1\cos u\sin 2i - 4\tilde{x}_1\sin u\sin 2i + \tilde{z}_1(3+\sin^2 i(5\cos^2 u - 7))\right)
\end{aligned}
\tag{31}
$$

Equation (31) describes the leading-order contribution of the differential inertial acceleration to the right-hand side of Equation (25).

Rotating Reference Frame Next, consider the perturbed equations of motion with respect to the RTN frame rotating with the chief's orbit,

$$
{}^{L}\boldsymbol{\delta}\ddot{\mathbf{r}} = -\mu\left(\frac{\mathbf{r}+\boldsymbol{\delta}\mathbf{r}}{\|\mathbf{r}+\boldsymbol{\delta}\mathbf{r}\|^3} - \frac{\mathbf{r}}{r^3}\right) + \mathbf{d}_I - 2\boldsymbol{\omega}\times\boldsymbol{\delta}\mathbf{v} - \dot{\boldsymbol{\omega}}\times\boldsymbol{\delta}\mathbf{r} - \boldsymbol{\omega}\times\boldsymbol{\omega}\times\boldsymbol{\delta}\mathbf{r} \tag{32}
$$

In addition to the disturbance's direct contribution to the dynamics through the differential acceleration $\mathbf{d}_I$, it has an indirect contribution through its effect on the angular velocity $\boldsymbol{\omega}$ of the frame itself. By definition, the RTN frame is rotating with the chief's orbit and a disturbance acting on the chief will create fictitious forces in this reference frame.

Beginning with the most rigorous definition for the angular velocity of the RTN basis attached to frame L with respect to the inertial frame I, and inserting a general perturbing force with components $\mathbf{f} = [f_R, f_T, f_N]^T$, we find

$$
\begin{aligned}
\boldsymbol{\omega} &= \left(\frac{{}^{I}d\hat{\mathbf{T}}}{dt}\cdot\hat{\mathbf{N}}\right)\hat{\mathbf{R}} + \left(\frac{{}^{I}d\hat{\mathbf{N}}}{dt}\cdot\hat{\mathbf{R}}\right)\hat{\mathbf{T}} + \left(\frac{{}^{I}d\hat{\mathbf{R}}}{dt}\cdot\hat{\mathbf{T}}\right)\hat{\mathbf{N}}\\
&= \left(\frac{f_N}{k}\sqrt{\frac{p}{\mu}}\right)\hat{\mathbf{R}} + \left(k^2\sqrt{\frac{\mu}{p^3}}\right)\hat{\mathbf{N}}
\end{aligned}
\tag{33}
$$

In the absence of perturbations, the angular velocity lies purely in the $\hat{\mathbf{N}}$ direction. An out-of-plane disturbance produces a radial component in the angular velocity vector, while an in-plane disturbance will affect the normal component of $\boldsymbol{\omega}$ through the parameters k and p. The fictitious forces also depend on the angular acceleration,

$$
\dot{\boldsymbol{\omega}} = \left(\frac{\dot{f}_N}{k}\sqrt{\frac{p}{\mu}} + \frac{e_x\sin u - e_y\cos u}{p}f_N - \frac{pf_Nf_T}{k^2\mu}\right)\hat{\mathbf{R}} + \left(\frac{k}{p}f_T - 2\mu\frac{k^3}{p^3}(e_x\sin u - e_y\cos u)\right)\hat{\mathbf{N}} \tag{34}
$$

In addition to the radial component of angular acceleration produced by a disturbance acting orthogonal to the orbit plane, an $\hat{\mathbf{N}}$ component is created by a disturbance acting in the along-track direction.

Substituting Equations (33) and (34) into the fictitious forces in Equation (32), normalizing the

coordinates, and performing the change of variables from time to argument of latitude, we obtain

$$\begin{aligned} d_{x,L}(u) &= \frac{p^2}{\mu k^3}\left(-f_N\tilde{z}_1 + f_T\tilde{y}_1\right) \\ d_{y,L}(u) &= \frac{p^2}{\mu k^3}\left(2f_N\tilde{z}' + \left(f'_N - 3\frac{k'}{k}f_N\right)\tilde{z}_1 - f_T\tilde{x}_1\right) \\ d_{z,L}(u) &= \frac{p^2}{\mu k^3}\left(-f_N\tilde{x}_1 - 2f_N\tilde{y}'_1 - \tilde{y}_1\left(f'_N - 3\frac{k'}{k}f_N\right)\right) \end{aligned} \tag{35}$$

Equation (35) gives the contribution of a general disturbance force to the right-hand side of Equation (25) due to fictitious forces arising from the rotating reference frame. Using Equation (28) for the force of J_2 expressed in the chief's RTN components, the disturbance becomes

$$\begin{aligned} d_{x,L}(u) &= -\frac{3J_2R_E^2}{p^2}k\left(-\tilde{z}_1\sin i\cos i\sin u + \tilde{y}_1\sin^2 i\sin u\cos u\right) \\ d_{y,L}(u) &= -\frac{3J_2R_E^2}{p^2}\left[\left(2k\tilde{z}'_1\sin u + \tilde{z}_1\left(k'\sin u + k\cos u\right)\right)\sin i\cos i - \tilde{x}_1\sin^2 i\sin u\cos u\right] \\ d_{z,L}(u) &= -\frac{3J_2R_E^2}{p^2}\left[-k(\tilde{x}_1 + 2\tilde{y}'_1)\sin u - \tilde{y}_1\left(k'\sin u + k\cos u\right)\right]\sin i\cos i \end{aligned} \tag{36}$$

Change of Variables The effects considered thus far arose from the equations of relative motion in the rotating frame of the chief. Those effects appear whether the independent variable is time, true anomaly, or argument of latitude. As noted above, the true anomaly can be a strong function of the perturbation for near-circular orbits. The argument of latitude is much less sensitive to the perturbation, but is not completely independent of it. Hence, there will be a correction to the equations of motion when derivatives are taken with respect to u.

The derivation of the TH equations makes use of the fact that for Keplerian motion, $\dot{f} = \dot{u} = \boldsymbol{\omega}\cdot\hat{\mathbf{N}} = k^2\sqrt{\mu/p^3}$. The last equality still holds in the presence of perturbations, as seen in Equation (33), but the first two do not. The evolution of the true anomaly and argument of latitude differ because the argument of perigee is no longer constant. Similarly, the argument of latitude rate differs from the normal component of angular velocity due to the evolution of right ascension of the ascending node Ω,

$$\dot{u} = k^2\sqrt{\frac{\mu}{p^3}} - \dot{\Omega}\cos i \tag{37}$$

where $\dot{\Omega}$ and the other orbital element rates are related to the perturbing acceleration by the Gauss Variational Equations (GVE).

The leading-order effects of the change of variables arise from the first-order dynamics of Equation (8). Smaller effects would arise from the higher-order Keplerian dynamics as well as transformation of the disturbances due to differential inertial acceleration and fictitious forces, but these are below the truncation threshold for this analysis. To change variables from time to argument of latitude, we employ relations of the form $\dot{x} = \dot{u}x'$ and $\ddot{x} = \dot{u}\dot{u}'x' + \dot{u}^2x''$ and divide by $\dot{u}^2$ to isolate x''. Using the binomial series to expand $\dot{u}^{-1}$ and $\dot{u}^{-2}$ and truncating at first-order in the

perturbation-dependent $\dot{\Omega}$, the equations of motion become

$$\begin{aligned}
\begin{bmatrix} \tilde{x}'' \\ \tilde{y}'' \\ \tilde{z}'' \end{bmatrix} \approx & \begin{bmatrix} \frac{3}{k}\tilde{x} + 2\tilde{y}' \\ -2\tilde{x}' \\ -\tilde{z} \end{bmatrix} + \frac{1}{k^2}\sqrt{\frac{p^3}{\mu}} \begin{bmatrix} \tilde{x}\frac{6\dot{\Omega}\cos i}{k^2} + 2\tilde{y}'\dot{\Omega}\cos i \\ -2\tilde{x}'\dot{\Omega}\cos i \\ -2\tilde{z}\dot{\Omega}\cos i \end{bmatrix} \\
& + \frac{1}{k^2}\sqrt{\frac{p^3}{\mu}} \left\{ \frac{1}{2k}\left(3\left(e_x \sin u - e_y \cos u\right)\dot{\Omega}\cos i - \dot{e}_x \cos u - \dot{e}_y \sin u\right) + \dot{\Omega}'\cos i \right\} \begin{bmatrix} \tilde{x}' \\ \tilde{y}' \\ \tilde{z}' \end{bmatrix} \\
& + \frac{1}{k^3}\sqrt{\frac{p^3}{\mu}} \left\{ \dot{\Omega}\cos i \left(\frac{(e_x \sin u - e_y \cos u)^2}{2k} + k - 1 \right) \right. \\
& \left. + \frac{e_x \sin u - e_y \cos u}{2k}\left(\dot{e}_x \cos u + \dot{e}_y \sin u\right) - \dot{e}_x \sin u + \dot{e}_y \cos u \right\} \begin{bmatrix} \tilde{x} \\ \tilde{y} \\ \tilde{z} \end{bmatrix}
\end{aligned} \tag{38}$$

The first term on the right-hand side of Equation (38) appears in the unperturbed TH equations. The remaining terms represent the leading-order effects of the disturbance introduced by the change of variables. These can be related back to the RTN components of the perturbing force by using the GVE to substitute for $\dot{\Omega}$, $\dot{e}_x$, $\dot{e}_y$, and $\dot{\Omega}'$. The latter is the derivative of $\dot{\Omega}$ with respect to u, neglecting variations in the other orbital elements which only contribute to higher-order effects.

For J_2 perturbation, the contribution to the disturbance in Equation (25) is

$$\begin{aligned}
d_{x,\dot{u}}(u) = & \frac{3J_2R_E^2}{2p^2}\left(\left(-12\cos^2 i \sin^2 u + k(1 - 3\sin^2 i \sin^2 u)\right)\tilde{x}_1 - 4k\tilde{y}_1' \cos^2 i \sin^2 u \right. \\
& \left. - \left(2(1 + 2\cos 2i)k\cos u - (1 + \cos 2i)(e_x + \cos u)\right)\tilde{x}_1' \sin u\right) \\
d_{y,\dot{u}}(u) = & \frac{3J_2R_E^2}{2p^2}\left(k(1 - 3\sin^2 i \sin^2 u)\tilde{y}_1 + 4k\tilde{x}_1' \cos^2 i \sin^2 u \right. \\
& \left. - \left(2(1 + 2\cos 2i)k\cos u - (1 + \cos 2i)(e_x + \cos u)\right)\tilde{y}_1' \sin u\right) \\
d_{z,\dot{u}}(u) = & \frac{3J_2R_E^2}{2p^2}\left(k(1 + (4 - 7\sin^2 i)\sin^2 u)\tilde{z}_1 \right. \\
& \left. - \left(2(1 + 2\cos 2i)k\cos u - (1 + \cos 2i)(e_x + \cos u)\right)\tilde{z}_1' \sin u\right)
\end{aligned} \tag{39}$$

Modified First-Order Dynamics The combined contributions of differential inertial acceleration, fictitious forces in the rotating frame, and corrections to the change of variables provide an accurate model of the leading-order effects of perturbation when using the osculating chief orbital elements. However, it is desirable to use mean orbital elements which are constant or slowly-varying, especially when integrating the system of equations to obtain a solution.[29] One additional leading-order effect arises from the use of mean orbital elements. The first-order dynamics in Equation (8) depend upon the state variables as well as the parameter $k = 1 + e_x \cos u + e_y \sin u$. The difference between osculating and mean values of e_x and e_y constitutes a first-order effect of the perturbation on the equations of motion. To account for this difference, let $e_x = \bar{e}_x + \Delta e_x$ and $e_y = \bar{e}_y + \Delta e_y$. Taking the binomial series expansion of k^{-1} in the small quantities Δe_x and Δe_y, substituting into the TH equations, and truncating at first order, we obtain the disturbance

$$d_{x,k}(u) = -3\frac{\Delta e_x \cos u + \Delta e_y \sin u}{k^2}\tilde{x}_1 \tag{40}$$

Note that k in the denominator is computed using the mean orbital elements, as in the rest of the disturbance equations. Recalling the definitions of e_x and e_y, we can further expand to produce

$$\begin{aligned} \Delta e_x &= \Delta e \cos\omega - e\Delta\omega \sin\omega \\ \Delta e_y &= \Delta e \sin\omega + e\Delta\omega \cos\omega \end{aligned} \tag{41}$$

The appendix provides expressions for Δe and $\Delta\omega$ for the J_2 perturbation, based on the theory of Brouwer and Lyddane.[30] While the mean elements of both the chief and deputy give a complete description of the relative motion, the model being developed in this work assumes no knowledge of the deputy's absolute orbit and characterizes the relative motion using only parameters of the chief's orbit and relative position and velocity observables.

The total disturbances that must be added to the right-hand side of Equation (25) are

$$\begin{aligned} d_x(u) &= d_{x,I}(u) + d_{x,L}(u) + d_{x,\dot{u}}(u) + d_{x,k}(u) \\ d_y(u) &= d_{y,I}(u) + d_{y,L}(u) + d_{y,\dot{u}}(u) \\ d_z(u) &= d_{z,I}(u) + d_{z,L}(u) + d_{z,\dot{u}}(u) \end{aligned} \tag{42}$$

with the terms on the right given by Equations (31), (36), (39), and (40).

Partial Solution

Using the combined disturbance expressions in Equation (42) as $RHS_i(u)$ in Equation (13), the system can be solved by the procedure outlined in Equations (14) through (19). The only modifications necessary are the use of the homogeneous solutions ψ_1 and ψ_2 defined in Equation (21), rather than φ_1 and φ_2 of Equation (17), and integration with respect to u rather than f. While this variation of parameters approach reduces the problem of solving the equations of motion to the evaluation of integrals, it does not guarantee that the integrals have clean analytical expressions. Unlike the higher-order Keplerian corrections in both Cartesian and spherical coordinates, the disturbance expressions for Earth oblateness perturbation do not give rise to integrals that can be readily evaluated. However, a partial solution has been obtained.

Recall that corrections developed through the method of successive approximations are built upon the first-order solution, and therefore expressed as functions of the integration constants K_1 through K_6. Only a subset of the constants lead to difficult integrals, specifically K_1, K_2, and K_3 in the in-plane components of the relative motion. These approximately represent differences in semimajor axis and eccentricity vectors between the two spacecraft. Solutions for the effects of K_4, K_5, and K_6, which represent along-track offset and relative inclination, on $\tilde{x}$ and $\tilde{y}$ have been derived. These are given by

$$\begin{aligned} \tilde{x}_{J_2,4} &= -3K_4J_2\left(\frac{R_E}{p}\right)^2 \sin^2 i \left[\frac{1}{3}k\sin u\cos u + c_{xj4}\left(1+\frac{3}{2}kk'J(t)\right) + c_{xs4}k\sin u + c_{xc4}k\cos u\right] \\ \tilde{x}_{J_2,5} &= -3K_5J_2\left(\frac{R_E}{p}\right)^2 \sin i\cos i \left[-\frac{1}{3}k(1+\cos^2 u) + c_{xj5}\left(1+\frac{3}{2}kk'J(t)\right) + c_{xs5}k\sin u + c_{xc5}k\cos u\right] \\ \tilde{x}_{J_2,6} &= -3K_6J_2\left(\frac{R_E}{p}\right)^2 \sin i\cos i \left[\frac{1}{3}k\sin u\cos u + c_{xj6}\left(1+\frac{3}{2}kk'J(t)\right) + c_{xs4}k\sin u + c_{xc4}k\cos u\right] \end{aligned} \tag{43}$$

$$
\begin{aligned}
\tilde{y}_{J_2,4} &= -3K_4J_2\left(\frac{R_E}{p}\right)^2\sin^2 i\left[\frac{1}{3}\left(\frac{1}{2}(\sin^2 u-\sin^2 u_0)-e_x(\cos u-\cos u_0)+e_y(\sin u-\sin u_0)\right)\right.\\
&\quad\left.-\,c_{xj4}\frac{3}{2}k^2J(t)+c_{xs4}\left((1+k)\cos u-(1+k_0)\cos u_0\right)-c_{xc4}\left((1+k)\sin u-(1+k_0)\sin u_0\right)\right]\\
\tilde{y}_{J_2,5} &= -3K_5J_2\left(\frac{R_E}{p}\right)^2\sin i\cos i\left[-\frac{1}{3}\left((k+1)\sin u\cos u-(k_0+1)\sin u_0\cos u_0\right)\right.\\
&\quad+e_x(\sin u-\sin u_0)-2e_y(\cos u-\cos u_0)+2(u-u_0)-c_{xj5}\frac{3}{2}k^2J(t)\\
&\quad\left.+\,c_{xs5}\left((1+k)\cos u-(1+k_0)\cos u_0\right)-c_{xc5}\left((1+k)\sin u-(1+k_0)\sin u_0\right)\right]\\
\tilde{y}_{J_2,6} &= -3K_6J_2\left(\frac{R_E}{p}\right)^2\sin i\cos i\left[\frac{1}{3}\left((k+1)\sin^2 u-(k_0+1)\sin^2 u_0\right)-\frac{2}{3}e_x(\cos u-\cos u_0)\right.\\
&\quad+\frac{1}{3}e_y(\sin u-\sin u_0)-c_{xj6}\frac{3}{2}k^2J(t)+c_{xs6}\left((1+k)\cos u-(1+k_0)\cos u_0\right)\\
&\quad\left.-\,c_{xc6}\left((1+k)\sin u-(1+k_0)\sin u_0\right)\right]
\end{aligned}
\tag{44}
$$

where c_{xji}, c_{xsi}, and c_{xci} are constants given in the Appendix. The leading-order J_2 correction to the out-of-plane $\tilde{z}$ component, including effects from all integration constants, is given by

$$
\begin{aligned}
\tilde{z}_{J_2} &= 3J_2\left(\frac{R_E}{p}\right)^2\left\{\left[\sin i\cos i\left(\frac{2}{3}K_1+K_2e_y+K_3e_x\right)+\frac{1}{3}K_5\sin^2 i\right](1-k)(\sin u-\sin u_0)\right.\\
&\quad+\left[\sin i\cos i\left(\frac{4}{3}K_2e_y+\frac{1}{3}K_2+2K_2e_y^2+2K_3e_xe_y-\frac{1}{3}K_4e_x\right)+\frac{2}{3}K_5e_y\sin^2 i\right](1-\cos(u-u_0))\\
&\quad+\left[\sin i\cos i\left(\frac{1}{3}K_1(2k_0+1)+(K_2e_y+K_3e_x)(k_0+1)+\frac{1}{3}(K_2\sin u_0+K_3\cos u_0)\right)\right.\\
&\quad\left.+\frac{1}{6}K_5\sin^2 i(2k_0+1)+\cos^2 i(K_5\sin u_0+K_6\cos u_0)k_0\sin u_0\right]\cos u_0\sin(u-u_0)\\
&\quad-\left[\sin i\cos i\,(K_1+2(K_2e_y+K_3e_x))+\frac{1}{2}K_5\sin^2 i\right](u-u_0)\cos u\\
&\quad+\frac{1}{3}\sin i\cos i\,[K_2(\cos u-\cos u_0)-K_3(\sin u-\sin u_0)]\cos u\\
&\quad+\frac{1}{3}\left(K_4\sin i\cos i+K_6\cos^2 i\right)[(1-k)(\cos u-\cos u_0)+(1-k_0)\sin u_0\sin(u-u_0)]\\
&\quad+\cos^2 i\left[-\frac{1}{3}(K_5e_y+K_6e_x)\sin u(\sin u-\sin u_0)-\frac{1}{3}K_6(k-k_0)\cos u\right.\\
&\quad\left.\left.+\frac{1}{6}(K_5\sin u+K_6\cos u)\left((2k+1)\cos^2 u-(2k_0+1)\cos^2 u_0\right)\right]\right\}
\end{aligned}
\tag{45}
$$

Equations (43), (44), and (45) provide the leading-order J_2 corrections and can be added directly to the YA solution, combined with the higher-order Keplerian solutions, or with corrections for other orbit perturbations. The relative velocity components can be computed by differentiation of the corresponding relative position component with respect to true anomaly, but do not contribute any additional solution information and are therefore omitted here. The next section will demonstrate the improvement in accuracy achieved by different correction combinations, as well as what could be achieved by a complete solution to the disturbance model developed in this section.

Table 1. Chief Orbit Parameters for Performance Comparison Scenarios

h_p (km)	i_c	Ω_c	ω_c	f_0
750	98°	30°	30°	0°

VALIDATION

To demonstrate the validity of the J_2 disturbance equations and partial solution, we evaluate their predictions against the fundamental orbital differential equation subject to the J_2 perturbation given in Equation (27). First we will examine a representative scenario to provide a concrete example, then widen the discussion to broader trends. This analysis uses the osculating orbital elements listed in Table 1 to initialize the chief's absolute orbit. To distinguish between complete and incomplete components of the perturbation solution, the integration constants $\mathbf{K}$ are used to initialize the relative state through Equation (10).

As an illustrative example, consider a chief spacecraft in near-circular orbit with $e_c = 0.001$, and a deputy whose motion relative to the chief is characterized by $a\mathbf{K} = [0.1, 2, 2, 5, 2, -2]^T$ km. Thus, there will be an along-track drift due to the difference in semimajor axis indicated by K_1, periodic in-plane motion driven by the nonzero values of K_2 and K_3, an initial along-track offset of 5 km due to K_4, and periodic out-of-plane motion caused by K_5 and K_6. Figure 1 shows the deputy's trajectory in the chief's RTN coordinate frame as predicted by the J_2-perturbed truth model and by the combined second-order and partial J_2 solutions. For this assessment, care has been taken to ensure that the evaluation of the J_2 correction equations is consistent with the assumptions applied in solving them. In particular, mean values of a, e, and i, and the initial mean value of ω are used. For comparison, the Figure 1 also shows the trajectories predicted by the WLD model without J_2 corrections, and by the Butcher-Burnett solution for J_2-perturbed, near-circular orbits. All three models exhibit the qualitative behavior described above, but there is a growing discrepancy between the approximate analytical propagations and the truth model.

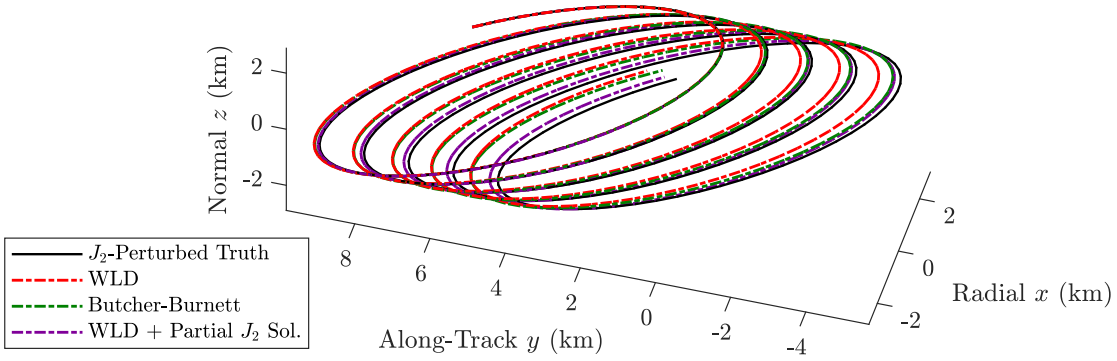

Figure 1. Relative Trajectory in RTN Frame with $e_c = 0.001$ and $a\mathbf{K} = [0.1, 2, 2, 5, 2, -2]^T$ km.

A more quantitative comparison of the propagation error is provided by Figure 2, which breaks the relative position error into its components in the radial, along-track, and normal directions. In addition to the three approximate models shown in Figure 1, it includes four closely-related models. Among these are the first-order YA and Schweighart-Sedwick solutions, which include eccentric-

ity effects and averaged J_2 perturbation, respectively. Another is a model that adds the partial J_2 corrections of Equations (43), (44), and (45) to YA, but neglects the second-order corrections of WLD. The last model combines the second-order Keplerian corrections of the WLD solution with a numerical integration of the complete equations describing the leading-order J_2 corrections, enumerated in Equation (42). For consistency with the analytical results, the integration is performed by substituting the first-order solution into Equations (31), (36), (39), and (40). Similarly, initial mean orbital elements are used everywhere except where the present mean value of $\bar{\omega}$ is needed to compute $\Delta\omega$ from Equation (41). Because $\bar{\omega}$ varies linearly in time, it can be readily computed without numerical integration and grows in proportion to $J(t)$. To distinguish it from the purely analytical solutions, this model is plotted as a solid line in a lighter shade.

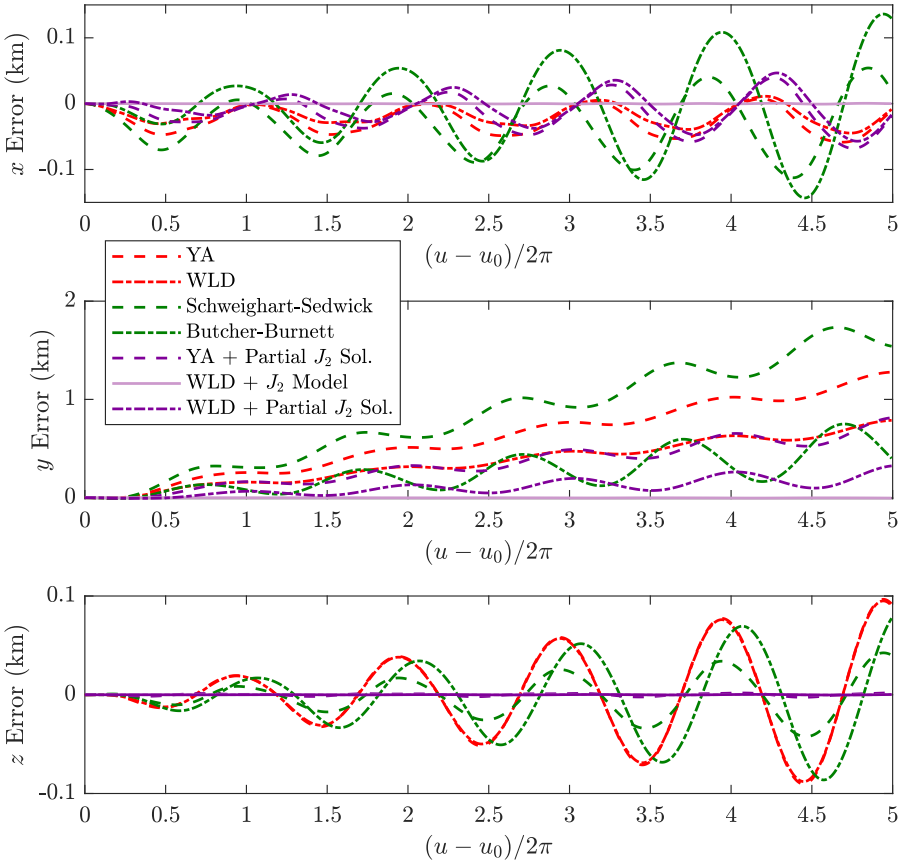

Figure 2. Error in Relative Trajectory Components with $e_c = 0.001$ and $a\mathbf{K} = [0.1, 2, 2, 5, 2, -2]^T$ km.

A few notable trends are on display in Figure 2. First, the error in the relative position for all models is dominated by drift in the along-track y component. Whereas errors in x and z remain on the order of a few tens of meters, the errors in y grow to hundreds of meters over a few orbits for most of the models shown. Incorporating the partial J_2 solution into the YA and WLD models improves the accuracy mainly by reducing the along-track error. Furthermore, adding either the J_2 or second-order Keplerian corrections to the YA solution results in very similar improvement for this scenario, while adding both leads to a considerably more accurate model. However, the

numerical integration results show that much further improvement could be achieved in the accuracy of the in-plane motion with a complete solution. In contrast, the analytical model with second-order corrections is identical to the numerical integration for the out-of-plane motion because a complete solution for the leading-order J_2 effects on z is given by Equation (45).

The major contribution of this work is the development of a J_2 perturbation model and analytical solution applicable to elliptical orbits. Figure 3 demonstrates this applicability by comparing propagation errors across a range of orbit eccentricities. This analysis uses the same parameters as the example above to initialize the absolute and relative motion, but averages the error in the relative position vector over the fifth orbit to condense the propagation accuracy for a given scenario into a representative point. As expected, the two models in green that assume circular orbits give better performance when the eccentricity is very small. In this limit, the Schweighart-Sedwick model is slightly more accurate than the first-order Yamanaka-Ankersen solution that neglects J_2 entirely. However, both the Schweighart-Sedwick and Butcher-Burnett solutions lose accuracy when the eccentricity is greater than about 0.001, the traditional threshold for "near-circular" orbits. In contrast, the solutions based on the TH equations–YA and WLD–are insensitive to eccentricty variations unless the orbit is highly elliptical. As seen in Figure 2, adding the partial J_2 correction to the YA solution improves its accuracy to the level of the second-order Keplerian WLD solution. If the second-order Keplerian effects are also included, the accuracy is better than the Butcher-Burnett solution even at very low eccentricities.

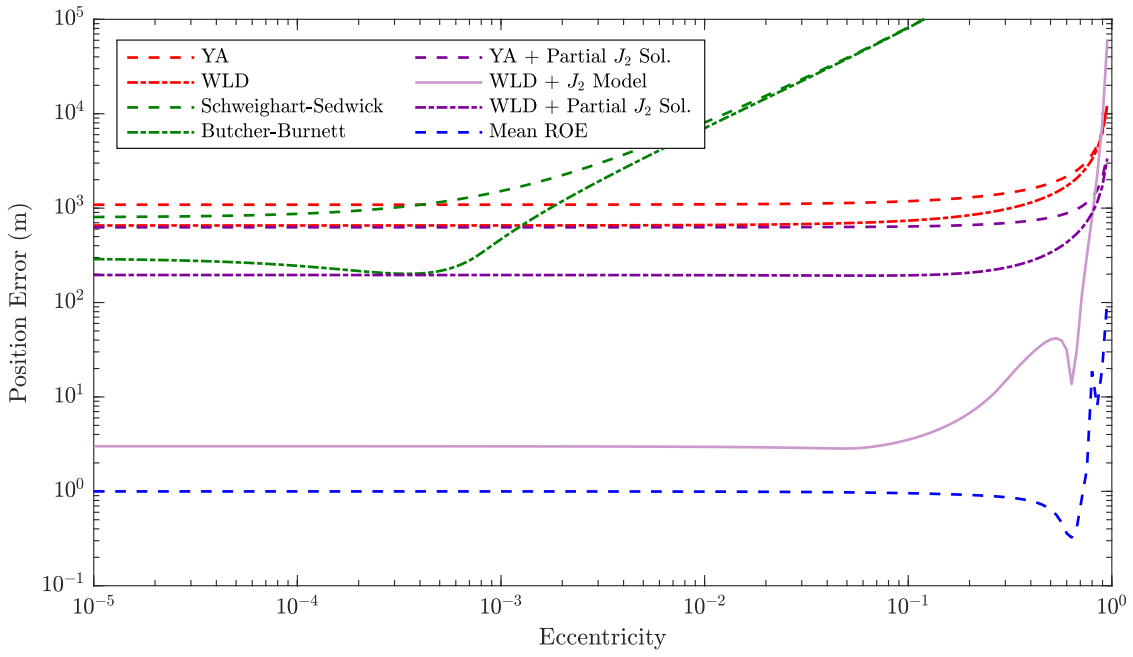

Figure 3. Average Position Error for a Range of Eccentricities with $a\mathbf{K} = [0.1, 2, 2, 5, 2, -2]^T$ km.

A striking feature of Figure 3 is the large gap between the analytical solutions and the numerically integrated model represented by the solid line. Whereas the linear error scale of Figure 2 masks the differences between the more accurate models, these are on full display when the error is presented on a logarithmic scale. The complete leading-order J_2 model is nearly two orders of

magnitude more accurate than the partial analytical solution combined with WLD. This suggests that substantial improvement could be achieved by developing exact or approximate solutions for the effects of the other integration constants on the in-plane motion. To contextualize the accuracy of the new J_2 model, the figure includes a propagation based on mean ROE. This uses an exact analytical conversion from the absolute position and velocity of the chief and deputy to their osculating and mean orbital elements. The latter are combined into ROE and propagated according to a linearization of the GVE, then converted back to absolute and relative position vectors for error analysis. The mean ROE model is slightly more accurate than the new J_2 model based on relative position coordinates, but neglects potential compounding of errors in the transformations between intermediate state parameters.

As a final test, we repeat the analysis of Figure 3 for a case where only the three integration constants with complete J_2 solutions in Equations (43) and (44) are excited. Figure 4 shows the relative position error as a function of the chief's eccentricity when $K_1 = K_2 = K_3 = 0$ in the initialization of the relative state. The distribution of the solutions is similar to the previous comparison, except that now the partial analytical solution is identical to the numerically integrated model combined with WLD. This verifies that the solutions presented in Equations (43) and (44) are the correct solutions to the in-plane disturbance equations involving K_4, K_5, and K_6.

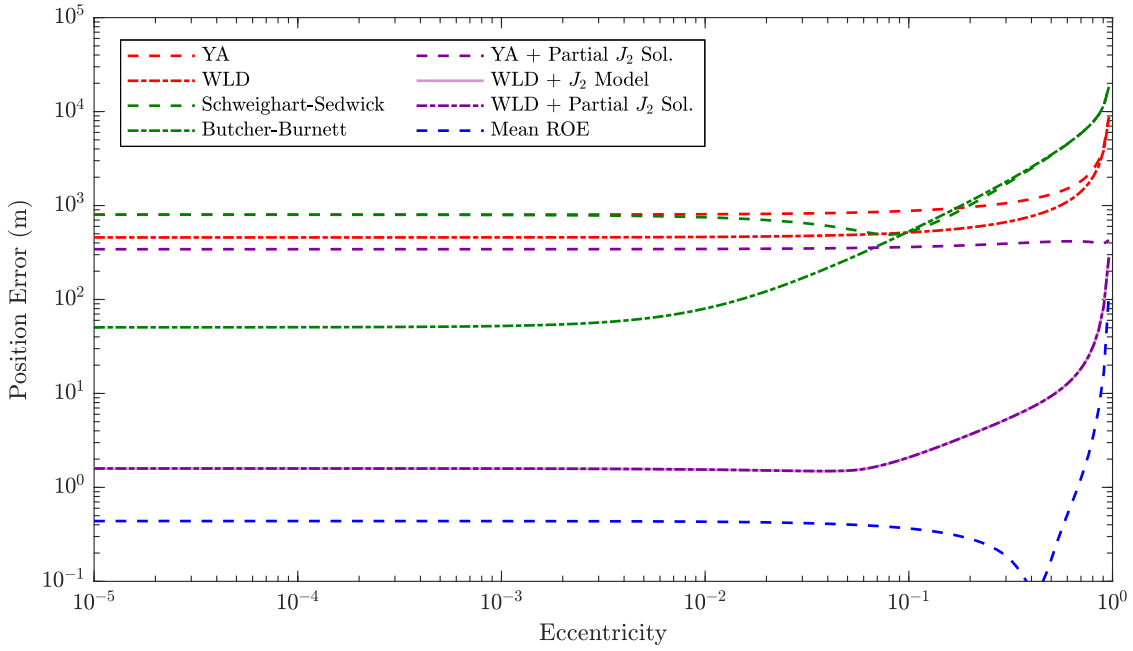

Figure 4. Average Position Error for a Range of Eccentricities with $a\mathbf{K} = [0, 0, 0, 5, 2, -2]^T$ km.

CONCLUSION

This work addressed the need for accurate and efficient models of spacecraft relative motion with the introduction of a framework for incorporating general perturbations into higher-order solutions for eccentric orbits, and its application to J_2. Perturbation effects manifest in the relative dynamics in four distinct ways: through the differential inertial force acting on the formation, through the

perturbation of the rotating reference frame in which the motion is described, through the change of independent variable from time to argument of latitude to handle eccentricity, and finally through the effect of the osculating orbital elements on the coordinate normalization. A partial solution to the J_2 disturbance equations has been presented, which captures all leading-order effects on the out-of-plane component and effects from three of the six integration constants on the in-plane components.

The validity of the model was demonstrated across a wide range of orbit eccentricities. It was found that the incorporation of both second-order Keplerian and leading-order J_2 effects was necessary to achieve a significant improvement in accuracy, a result consistent with the intuition that these effects are of comparable magnitude in low Earth orbit. The partial J_2 solution was evaluated against a numerical integration of the disturbance equations and shown to be correct in scenarios where only the relevant integration constants were nonzero. In scenarios in which all relative motion modes were excited, the propagation error could be reduced by an order of magnitude or more if a complete solution to the J_2 disturbance equations was available.

The developments in this work open many interesting paths for future research. Although this paper examines only the J_2 perturbation, the general framework presented herein could be used to analytically model the effects of other perturbations as well as spacecraft control actions. Furthermore, the framework was derived in the context of the Cartesian relative state and should be extended to curvilinear coordinates. Because it is linear in the relative position and velocity components, it may take on the same or a very similar form in spherical or cylindrical coordinates, just as the first-order Keplerian dynamics do. Beyond such investigations into the dynamics, the high-fidelity analytical models should be used to address problems of practical interest. One such application would be initial relative orbit determination using bearing angle measurements from a single camera. This problem is sensitive to dynamics modeling errors and typically requires observations over a large fraction of an orbit. However, a highly accurate analytical solution for the relative position could enable angles-only orbit determination from a very short measurement arc. By reducing the time and computational cost of such navigation and control tasks, high-fidelity analytical models will enable greater autonomy in future formation flying missions.

ACKNOWLEDGMENTS

This work was supported by the NASA Office of the Chief Technologist's Space Technology Research Fellowship, NASA grant number 80NSSC18K1176. The authors would also like to thank Eric Butcher and Ethan Burnett for providing the code for their higher-order solutions.

REFERENCES

[1] S. D'Amico, M. Pavone, S. Saraf, A. Alhussien, T. Al-Saud, S. Buchman, R. Bryer, and C. Farhat, "Distributed Space Systems for Future Science and Exploration," 8th International Workshop on Spacecraft Formation Flying, Delft University, June 8-10, 2015.

[2] J. Sullivan, S. Grimberg, and S. D'Amico, "Comprehensive Survey and Assessment of Spacecraft Relative Motion Dynamics Models," *Journal of Guidance, Control, and Dynamics*, Vol. 40, No. 8, 2017, pp. 1837–1859.

[3] W. H. Clohessy and R. S. Wiltshire, "Terminal Guidance System for Satellite Rendezvous," *Journal of Guidance, Control, and Dynamics*, Vol. 27, No. 9, 1960, pp. 653–658.

[4] H. S. London, "Second Approximation to the Solution of the Rendezvous Equations," *AIAA Journal*, Vol. 1, No. 7, 1963, pp. 1691–1693.

[5] M. L. Anthony and F. T. Sasaki, "Rendezvous Problem for Nearly Circular Orbits," *AIAA Journal*, Vol. 3, No. 7, 1965, pp. 1666–1673.

[6] M. T. Stringer, B. A. Newman, T. A. Lovell, and A. Omran, "Analysis of a New Nonlinear Solution of Relative Orbital Motion," 23rd International Symposium on Space Flight Dynamics, Pasadena, California, October 29-November 2, 2012.

[7] B. A. Newman, A. J. Sinclair, T. A. Lovell, and A. Perez, "Comparison of Nonlinear Analytical Solutions for Relative Orbital Motion," AAS/AIAA Astrodynamics Specialist Conference, San Diego, California, August 4-7, 2014.

[8] R. G. Melton, "Time-Explicit Representation of Relative Motion Between Elliptical Orbits," *Journal of Guidance, Control, and Dynamics*, Vol. 23, No. 4, 2000, pp. 604–610.

[9] E. A. Butcher, T. A. Lovell, and A. Harris, "Third Order Cartesian Relative Motion Perturbation Solutions for Slightly Eccentric Chief Orbits," 26th AAS/AIAA Space Flight Mechanics Meeting, Napa, CA, February 14-18, 2016.

[10] J. Tschauner and P. Hempel, "Optimale Beschleunigungsprogramme fur das Rendezvous-Manover," *Astronautica Acta*, Vol. 10, No. 5-6, 1964, p. 296.

[11] T. E. Carter, "State Transition Matrices for Terminal Rendezvous Studies: Brief Survey and New Example," *Journal of Guidance, Control, and Dynamics*, Vol. 21, No. 1, 1998, pp. 148–155.

[12] K. Yamanaka and F. Ankersen, "New State Transition Matrix for Relative Motion on an Arbitrary Elliptical Orbit," *Journal of Guidance, Control, and Dynamics*, Vol. 25, No. 1, 2002, pp. 60–66.

[13] M. Willis, T. A. Lovell, and S. D'Amico, "Second Order Analytical Solution for Relative Motion on Arbitrarily Eccentric Orbits," 29th AAS/AIAA Space Flight Mechanics Meeting, Ka'anapali, Maui, Hawaii, January 13-17, 2019.

[14] M. Willis, K. T. Alfriend, and S. D'Amico, "Second-Order Solution for Relative Motion on Eccentric Orbits in Curvilinear Coordinates," AAS/AIAA Astrodynamics Specialist Conference, Portland, ME, August 11-15, 2019.

[15] T. Henderson, T. A. Lovell, A. Sizemore, K. Horneman, and D. Zuehlke, "Initial Relative Orbit Determination Solutions Using Polynomial Systems," 29th AAS/AIAA Space Flight Mechanics Meeting, Ka'anapali, Maui, HI, January 13-17, 2019.

[16] M. Willis and S. D'Amico, "Applications and Limitations of Angles-Only Relative Navigation Using Polynomial Solutions," AAS/AIAA Astrodynamics Specialist Conference, South Lake Tahoe, CA, August 9-13, 2020.

[17] D. A. Vallado, *Fundamentals of Astrodynamics and Applications*. Springer, 2007.

[18] D.-W. Gim and K. T. Alfriend, "State Transition Matrix of Relative Motion for the Perturbed Noncircular Reference Orbit," *Journal of Guidance, Control, and Dynamics*, Vol. 26, No. 6, 2003, pp. 956–971.

[19] A. W. Koenig, T. Guffanti, and S. D'Amico, "New State Transition Matrices for Relative Motion of Spacecraft Formations in Perturbed Orbits," AAS/AIAA Astrodynamics Specialist Conference, Long Beach, CA, September 13-16, 2016.

[20] B. Kuiack and S. Ulrich, "Nonlinear Analytical Equations of Relative Motion on J2-Perturbed Eccentric Orbits," *Journal of Guidance, Control, and Dynamics*, Vol. 41, No. 12, 2018, pp. 2664–2675.

[21] P. Gurfil and K. V. Kholshevnikov, "Manifolds and Metrics in the Relative Spacecraft Motion Problem," *Journal of Guidance, Control, and Dynamics*, Vol. 29, No. 4, 2006, pp. 1004–1010.

[22] S. A. Schweighart and R. J. Sedwick, "High-Fidelity Linearized J2 Model for Satellite Formation Flight," *Journal of Guidance, Control, and Dynamics*, Vol. 25, No. 6, 2002, pp. 1073–1080.

[23] S. A. Schweighart and R. J. Sedwick, "Cross-Track Motion of Satellite Formations in the Presence of J2 Disturbances," *Journal of Guidance, Control, and Dynamics*, Vol. 28, No. 4, 2005, pp. 824–826.

[24] A. Biria and R. Russell, "A Satellite Relative Motion Model Including J2 and J3 via Vinti's Intermediary," 26th AAS/AIAA Space Flight Mechanics Meeting, Napa, CA, February 14-18, 2016.

[25] E. A. Butcher, E. Burnett, J. Wang, and T. A. Lovell, "A New, Time-Explicit J2-Perturbed Nonlinear Relative Orbit Model with Perturbation Solutions," AAS/AIAA Astrodynamics Specialist Conference, Stevenson, WA, August 20-24 2017.

[26] E. Burnett, E. A. Butcher, A. J. Sinclair, and T. A. Lovell, "Linearized Relative Orbital Motion Model About an Oblate Body Without Averaging," AAS/AIAA Astrodynamics Specialist Conference, Snowbird, Utah, August 19-23, 2018.

[27] J. Sullivan and S. D'Amico, "Nonlinear Kalman Filtering for Improved Angles-Only Navigation Using Relative Orbital Elements," *Journal of Guidanced, Control, and Dynamics*, Vol. 40, No. 9, 2017, pp. 2183–2200.

[28] W. E. Boyce and R. C. DiPrima, *Elementary Differential Equations*. Wiley, 2008.

[29] K. T. Alfriend, S. R. Vadali, P. Gurfil, J. P. How, and L. S. Breger, *Spacecraft Formation Flying: Dynamics, control and navigation*. Elsevier, 2010.

[30] H. Schaub and J. L. Junkins, *Analytical Mechanics of Space Systems*. AIAA Education Series, 2nd ed., 2009.

APPENDIX A: SOLUTION COEFFICIENTS

The constant coefficients that appear in Equations (43) and (44) are listed below.

$$c_{xj4} = -2\frac{k_0^3 \sin u_0 \cos u_0}{1-e^2}$$
$$c_{xj5} = -4\frac{k_0^3 \sin^2 u_0}{1-e^2}$$
$$c_{xj6} = -4\frac{k_0^3 \sin u_0 \cos u_0}{1-e^2}$$

$$c_{xs4} = \frac{1}{3}\frac{\cos u_0}{1-e^2}\left[k_0^2 - 2k_0 + e_y^2 + e_y(k_0+2)\sin u_0 + (1+3k_0+3k_0^2)\sin^2 u_0\right]$$
$$c_{xs5} = \frac{1}{3}\frac{\sin u_0}{1-e^2}\left[(1-k_0)^2 - e_x^2 + 2e_y(2k_0+1)\sin u_0 + (1+6k_0+6k_0^2)\sin^2 u_0\right]$$
$$c_{xs6} = \frac{1}{3}\frac{\cos u_0}{1-e^2}\left[(1+4k_0+7k_0^2 + e_y^2 - (1+6k_0+6k_0^2)\cos^2 u_0 + e_y(4k_0+2)\sin u_0\right]$$

$$c_{xc4} = \frac{1}{3}\frac{\sin u_0}{1-e^2}\left[k_0^2 - 2k_0 + e_x^2 + e_x(k_0+2)\cos u_0 + (1+3k_0+3k_0^2)\cos^2 u_0\right]$$
$$c_{xc5} = \frac{1}{3}\frac{\cos u_0}{1-e^2}\left[2+8k_0+5k_0^2 - 3e_x^2 - 2e_y^2 - 2e_x(2k_0+1)\cos u_0 - (1+6k_0+6k_0^2)\cos^2 u_0\right] + \frac{2e_x k_0}{1-e^2}$$
$$c_{xc6} = \frac{1}{3}\frac{\sin u_0}{1-e^2}\left[1+4k_0+7k_0^2 + e_x^2 - (1+6k_0+6k_0^2)\sin^2 u_0 + e_x(4k_0+2)\cos u_0\right]$$

APPENDIX B: MEAN-TO-OSCULATING TRANSFORMATION FOR J2

Equation (41) uses the leading-order deviations from mean eccentricity and argument of perigee given by

$$\begin{aligned}
\Delta e = \frac{J_2}{16}\left(\frac{R_E}{p}\right)^2 (1-e^2)\Bigg[& e\left(1 - 11\cos^2 i - 40\left(\frac{\cos^4 i}{1-5\cos^2 i}\right)\right)\cos 2\omega \\
& + 4\left(\frac{3\cos^2 i - 1}{1-e^2}\left(e\sqrt{1-e^2} + \frac{e}{1+\sqrt{1-e^2}}\right)\right. \\
& + \left(3\frac{e}{1-e^2}\cos 2u - 3\cos(\omega+u) - \cos(3u-\omega)\right)\sin^2 i \\
& \left. + \left(\frac{3\cos^2 i - 1 + 3\sin^2 i\cos 2u}{1-e^2}\right)(1+k+k^2)\cos(u-\omega)\right)\Bigg] \\
\Delta\omega = \frac{J_2}{8}\left(\frac{R_E}{p}\right)^2 \Bigg\{ & \frac{\sqrt{1-e^2}}{e}\left[2(3\cos^2 i - 1)(k^2+k+1-e^2)\sin(u-\omega)\right. \\
& \left. + \sin^2 i\left(-3\left(k^2+k-(1-e^2)\right)\sin(\omega+u) + \left(3k(k+1) + (1-e^2)\right)\sin(3u-\omega)\right)\right] \\
& - \frac{1}{4}\left(2 + e^2 - 11(2+3e^2)\cos^2 i - 40(2+5e^2)\frac{\cos^4 i}{1-5\cos^2 i} - \frac{400e^2\cos^6 i}{(1-5\cos^2 i)^2}\right) \\
& - 6(1-5\cos^2 i)(u - (1-e^2)^{3/2}J(t) - (\omega + M_0) + e_x\sin u - e_y\cos u) \\
& (3-5\cos^2 i)\left(3\sin(2u) + 3e\sin(\omega+u) + e\sin(3u-\omega)\right)\Big\}
\end{aligned}$$